DISCHARGE MODELING OF LARGE SCALE LH2 EXPERIMENTS WITH AN ENGINEERING TOOL

Venetsanos A.G.[1*], Ustolin F.[1,2], Tolias I. [1], Giannissi S. [1], Momferatos G. [1], Coldrick S.[3], Atkinson G. [3], Lyons K. [3], Jallais S. [4]

[1]Environmental Research Laboratory, National Centre for Scientific Research "Demokritos", 15310 Aghia Paraskevi, Attikis, Greece, *venets@ipta.demokritos.gr

[2]Department of Mechanical and Industrial Engineering, Norwegian University of Science and Technology NTNU, Richard Birkelands vei 2B, 7034 Trondheim, Norway

[3]Health and Safety Executive, Harpur Hill, Buxton, Derbyshire, SK17 9JN, UK

[4]Air Liquide R&D / Campus Innovation Paris, 1 chemin de la Porte des Loges, 78350 Jouy-En-Josas, France

Keywords: LH_2, choked flow, discharge line effects, PIF algorithm, engineering tool

Abstract

Accurate estimation of mass flow rate and release conditions is important for the design of dispersion and combustion experiments, for the subsequent validation of CFD codes/models, for consequence assessment analysis within related risk assessment studies and for associated Regulation Codes and Standards development. This work focuses on the modelling of the discharge phase of the recent large scale LH2 release and dispersion experiments performed by HSE within the framework of PRESLHY project. The experimental conditions covered sub-cooled liquid stagnation conditions at two pressures (2 and 6 bara) and 3 release nozzle diameters (1, ½ and ¼ inches). The simulations were performed using a 1d engineering tool, which accounts for discharge line effects due to friction, extra resistance due to fittings and area change. The engineering tool uses the Possible Impossible Flow (PIF) algorithm for choked flow calculations and the Helmholtz Free Energy (HFE) EoS formulation. Three different phase distribution models were applied. The predictions are compared against measured and derived data from the experiments and recommendations are given both regarding engineering tool applicability and future experimental design.

1 INTRODUCTION

Accurate estimation of mass flow rate and release conditions is important for the design of dispersion and combustion experiments, for the subsequent validation of CFD codes/models, for consequence assessment analysis within related risk assessment studies and for associated Regulation Codes and Standards development.

In case of LH_2 releases earlier work [1] has shown that predicted mass flow rates for previous large scale LH_2 experiments exhibit medium to large overestimation with respect to reported experimental values. The scope of this work was to further analyse this deficiency using experimental data obtained during the new HSE large scale LH_2 tests performed within of PRESLHY EC-project, covering two tank stagnation pressures (2 and 6 bara), 3 nozzle diameters (1, ½ and ¼ inch) and various release orientations and heights, see [2,3].

For the present simulations the engineering tool developed earlier [1], which calculates choked flow with account of discharge line effects (friction and area change) using the Possible Impossible Flow (PIF) algorithm was extended to include extra flow resistance due to various fittings (valves, elbows, etc.) through either the (L/D)-equivalent method or the K-method. Along this line a full analysis of the resistances of the various sections of the discharge line of the new experiments was performed. Regarding phase distribution modelling along the discharge line, three different models were applied: a) the classical Homogeneous Equilibrium Mixture (HEM) model, b) a Homogeneous Non Equilibrium Mixture (HNEM) model that assumes no vapour appearance along the line and all liquid in metastable state below the bimodal curve and c) the most simple constant density model, with density equal to the stagnation density.

2 MATHEMATICAL FORMULATION

2.1 Pipe flow equations with extra resistance terms

The steady state 1-d integrated over pipe cross section mass, momentum and energy conservation differential equations are:

$$\rho u A = GA = \dot{m} = ct \tag{1}$$

$$G du = -dP - \frac{G^2 dx}{2\rho}\left(\frac{f_D}{D} + \frac{K}{L}\right) \tag{2}$$

$$d\left(h + \frac{1}{2}\left(\frac{G}{\rho}\right)^2\right) = 0 \tag{3}$$

In the above equations *dx* is the step along the discharge line, *G* is the mass flux, *A* is the line cross section (generally variable along the line), ρ is the density, *h* is the static enthalpy, *D* is the diameter, f_D is the Darcy friction factor, *K* is the extra resistance due to fittings (valves, elbows, etc.) and *L* is the length over which the resistance factor *K* applies. Resistance factors are often related to the Darcy friction factor and an equivalent pipe length to diameter ratio as following:

$$K = f_D\left(\frac{L}{D}\right)_{equ} \tag{4}$$

For incompressible flow, resistance factors appear in the Bernoulli equation as given below, where subscripts 1, 2 denote upstream and downstream locations respectively.

$$\frac{\rho}{2}u_1^2 + P_1 = \frac{\rho}{2}u_2^2 + P_2 + \frac{\rho}{2}Ku_2^2 \tag{5}$$

When resistance factors are specified by element manufacturers (e.g. in the form of flow rate versus pressured drop specification data/charts), then Bernoulli equation can be used to derive pressure drop. When simultaneous measurements of pressure drop and mass flow rate are available from experiments, then Bernoulli equation can be used to derive resistance factors. Both approaches were applied in this work.

It should be noted that in the special case of area change Bernoulli equation above takes the following form, which shows that resistance factor in this case is extra to dynamic pressure change solely due to area change.

$$\Delta P_{12} = \frac{\dot{m}^2}{2\rho}\left(\frac{1}{A_2^2} - \frac{1}{A_1^2}\right) + \frac{K}{2}\rho u_2^2 = \frac{\dot{m}^2}{2\rho A_2^2}\left[K + 1 - \left(\frac{A_2}{A_1}\right)^2\right] \tag{6}$$

The case of pipe contraction which is of interest in this work has been investigated by various researchers. According to [4], *K* for sudden diameter contraction is given by:

$$K = \frac{1}{2}\left(1 - \frac{A_2}{A_1}\right) \tag{7}$$

Alternatively, according to Borda Carnot equation [5]:

$$K = \left(1 - \frac{A_2}{A_3}\right)^2, \quad \frac{A_3}{A_2} = 0.63 + 0.37\left(\frac{A_2}{A_1}\right)^3 \tag{8}$$

Here subscript 3 denotes the location of minimum area due to vena contracta phenomenon and is considered to occur in between locations 1 and 2. The correlation for the contraction coefficient A_3/A_2 originates from Weisbach measurements. The Borda Carnot equation gives mechanical losses due to sudden expansion from location 3 to location 2.

2.2 Physical properties and phase change modelling

Single phase physical properties and vapour liquid equilibrium (bimodal curve) were calculated using the Helmholtz Free Energy (HFE) EoS formulation for normal hydrogen following [6].

Phase change modelling was treated with three different models:

- HEM model
- Constant density model
- HNEM all liquid model

HEM model is the default model of the engineering tool. It is well known that HEM model may produce Mach number discontinuity when crossing the saturation line, see [7].

The constant density model, the simplest of all models, assumes that density is constant along the discharge line. It is here assumed that this constant density is equal to the stagnation density and that exit pressure is atmospheric. In this case the energy equation is not used in the calculations.

In the special HNEM model applied in this work, it is assumed that only liquid exists along the discharge line which can be sub-cooled or saturated or superheated. Superheated liquid properties are calculated from the liquid spinodal line at given pressure. This model does not produce Mach number discontinuity when crossing the saturation line. This model can be applied only if the calculated superheat is lower than the maximum superheat, for given pressure. This is true for the present experiments, since for the HFE EoS formulation, the liquid spinodal temperature of normal hydrogen at atmospheric pressure is 29.143 K (= 0.8793 T_{cr}), which corresponds to a saturation pressure of 6.986 bara, i.e. higher than the maximum set experimental pressure of 6 bara.

It should be noted here as a parenthesis, that the ratio of the liquid spinodal temperature at atmospheric pressure to the critical temperature depends on the EoS used, see [8], who provided the values 0.844 for Van der Waals, 0.895 for Redlich-Kwong, 0.943 for Soave and 0.948 for Peng-Robinson EoS formulations.

2.3 Choked flow calculations

Choked mass flow rates are calculated using the possible-impossible flow (PIF) algorithm. The algorithm is described in details in [1]. An alternative implementation of the same algorithm is given in [9].

3 HSE EXPERIMENTS

3.1 Experimental layout

The various elements comprising the discharge line, in order of increasing distance from the tank, as well as their dimensions are presented in Table 1. A sketch of the line downstream the mass flow meter is shown in Figure 1.

The LH_2 tank was equipped with a pressure control heating system. During operation LH_2 was sucked from the tank bottom then heated to become vapour and then returned as vapour back to the tank top part in order to keep the tank pressure constant. It should be noted that this system although independent to the one simultaneously extracting LH_2 for the experiments could potentially create convective patterns inside the tank that might affect (possibly reduce) LH_2 extraction rate during the tests.

Table 1: Discharge line geometry with elements along the line.

Discharge line element	Diameter (mm)	Length (m)	Distance from tank
Pipework and fittings inside tanker (1.5 line with 2 globe valves and 4x90° elbows)	45	2.5	2.5
Connector	45 to 25.4	0.0	2.5
Vacuum insulated flexible hose	25.4	20	22.5
Electrically isolated pipe	25.4	0.5	23.0
Mass flow meter (MFM) section	25.4	0.4	23.4
Globe valve section	25.4	0.6	24.0
Flexible hose	25.4	1.75	25.75
Nozzle	25.4 to 25.4 or 12.7 or 6.35	0.0	25.75

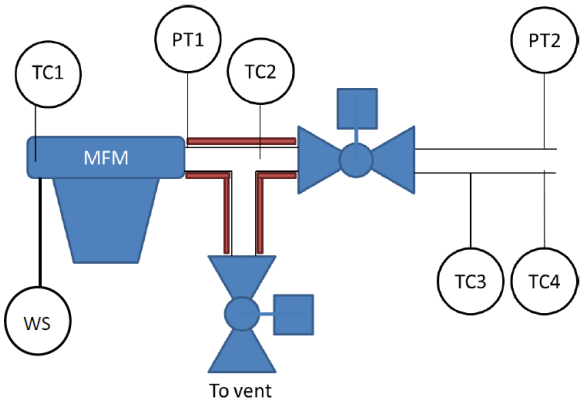

Figure 1: Sketch of last part (2.75 m) of the discharge line, including pressure transducers and thermocouples.

3.2 Pressure measurements

The experimental instrumentation included two pressure transducers PT1 and PT2, located just after the mass flow meter and 8 cm from the line exit respectively, see Figure 1. Table 2 shows the measured steady state values of pressure for tests 10, 11, 12 (all at 6 bara) with nozzle sizes 1, ½ and ¼ inch respectively.

Table 2: Pressure measurements for 6 bara tests.

Location	Distance from tank (m)	Measured Pressure (bara)		
		1 inch (test 10)	1/2 inch (test 11)	1/4 inch (test 12)
Tank	0	6	6	6
PT1	23.4	2.2	3.0	5.55
PT2	25.75	1.0	2.66	5.5

3.3 LH2 tank stagnation conditions

LH_2 storage pressure under normal conditions is usually a few kPa above atmospheric. Before starting any hydrogen release, LH_2 tank was pressurized fast to the experimental set stagnation pressure (2 or 6 bara) by activating the pressure control heating system. Experiments started soon after the set pressure was reached and LH_2 was pushed out from the tank bottom. The pressure control system was kept operating during the experimental release period to keep the set pressure constant. This fast pressurization procedure leads us to the conclusion that the stagnation conditions of the LH_2 pushed out from the bottom of the tank were sub-cooled at the set pressure.

For the simulations performed in this work, we assumed initial conditions before tank pressurization were saturated at 1.1 bara and that LH_2 pressurization from 1.1 bara to the set pressure was isentropic. Table 3 shows the calculated tank LH_2 stagnation conditions as calculated using the NCSRD engineering tool for physical properties and discharge simulation. It can noted that density changes are very small (density practically constant) during this pressurization.

Table 3: Tank LH2 stagnation conditions

P (bara)	T (K)	ρ (kg/m3)
1.1	20.650	70.524
2	20.695	70.597
6	20.893	70.915

3.4 Discharge line resistance factors

In this work K factors were estimated from Bernoulli equation based on the 6 bara, ½ inch nozzle tests for which HSE reported that the Coriolis mass flow meter steady reading of 265 g/s is the actual mass flow rate for these tests and corresponds to liquid flow up to the nozzle. A constant density equal to the LH_2 density at 1.1 bar (see Table 3) was used in the corresponding Bernoulli calculations. The following subsections present the estimations for each discharge line element separately.

3.4.1 Vacuum insulated flexible hose

It is known that flexible pipes create much higher resistance to the flow than rigid pipes, see [10]. Figure 2 (reproduction using hose manufacturer charts) shows the relation between pressure drop per pipe length and volume flow rate for LH2 for 1-inch pipes, where GMP in the figure refers to US gallons. Using a 70.85 kg/m^3 for LH2 density, friction factors for flexible and rigid pipes were estimated to be 0.145 and 0.01 respectively, i.e. the friction factor for the flexible pipe was found to be 14.5 times that of the rigid pipe.

The corresponding value of *K* for the 20 m flexible pipe is 114.17. Using the above resistance factor value, the measured liquid mass flow rate of 0.265 kg/s for test-11 and the density of liquid hydrogen at 1.1 bara, the pressure drop along the 20 m flexible pipe hose is estimated to be 2.22 bar.

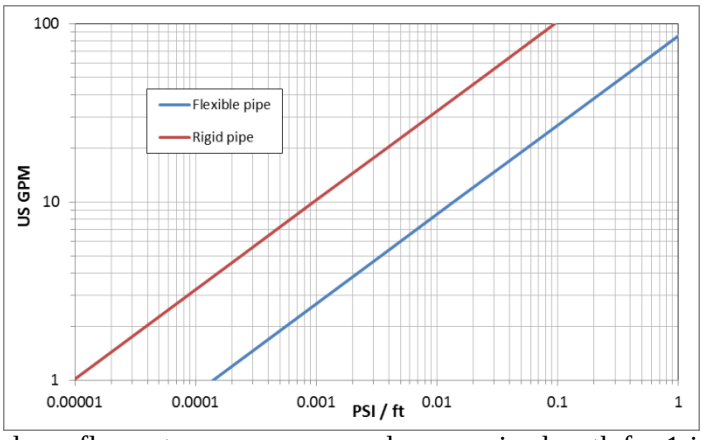

Figure 2: LH2 volume flow rate versus pressure drop per pipe length for 1-inch rigid and flexible piping, with friction factor = 0.145 for the flexible pipe and = 0.01 for the rigid pipe.

3.4.2 Electrically isolated pipe and Coriolis MFM section

HSE estimated 0.1 bar pressure drop for test-11 along the section containing the 0.5 m electrically isolated pipe followed by the 0.4 m Coriolis MFM. For test-11 this corresponds to a resistance factor K = 5.16.

3.4.3 Connection between tanker and flexible hose

The contraction from 45 mm to 25.4 mm in diameter leads to K = 0.34 according to Idelchik and K = 0.31 according to Borda Carnot. The larger Idelchik formulation is adopted here. This results into a total pressure drop of 0.02 bar across the area change for test-11 according to equation (6).

3.4.4 Tanker side

The sum of the pressure drops from LH2 tanker to transducer PT1 should be 3 bar according to the experimental data (Ptank – PT1) for test-11. Therefore the pressure drop inside the tanker up to the beginning of the contraction from tanker to flexible hose should be 0.66 bar. This results in a resistance factor K = 335.85 for test-11. For a usual value of $f_D = 0.02$, this gives $\left(\frac{L}{D}\right)_{eq} = 16793$, value which seems remarkably high, but could be attributed to the complexity of the discharge line within the tanker and possibly on the simultaneous operation of pressure control system.

3.4.5 Valve section and flexible hose before exit nozzle

The measured pressure drop (PT1-PT2) across the 0.6 m valve section and the 1.75 m flexible hose before the exit nozzle was 0.34 bar as reported in [2]. This corresponds to a resistance factor K = 17.53 for test-11.

3.4.6 The nozzle

The nozzle for test-11 is considered to consist of an abrupt contraction from 25.4 mm diameter to 12.7 mm diameter, followed by a very short pipe length, 12.7 mm in diameter. Assuming exit pressure of 1 bara as in [2], the total pressure drop across the nozzle is 1.66 bara (PT2-1.0 bara). This corresponds to K = 4.41 from equation (6), and a nozzle discharge coefficient $c_D = 0.432$, where:

$$c_D \equiv \frac{\dot{m}}{A_2\sqrt{2\rho\Delta P_{12}}} \tag{9}$$

3.4.7 Summary

Table 4 presents the estimated pressure distribution, and resistance factors K along the discharge line, for test-11. The sum of the pressure drops is 5 bars. Figure 3 shows the corresponding estimated pressure distribution. The figure also shows data for tests 10 (6 bara-1 inch) and 12 (6 bara-1/4 inch).

Table 4: Discharge line pressure distribution and resistance coefficients K for Test-11 (mass flow rate = 265 g/s, density 70.5 kg/m3).

Line elements in order	Diameter (mm)	Length (m)	Distance from tank	Pressure drop (bar)	Pressure (bara)	K
Tanker pipework	45	2.5	2.5	0.66	5.34	335.85
Contraction	45 to 25.4	0.0	2.5	0.02	5.32	0.34
Vacuum insulated flexible hose	25.4	20	22.5	2.22	3.10	114.17
Electrically isolated pipe + MFM	25.4	0.9	23.4	0.10	3.00	5.16
Valve section + Flexible hose	25.4	2.35	25.75	0.34	2.66	17.53
Nozzle	25.4 to 12.7	0.0	25.75	1.66	1.00	4.41

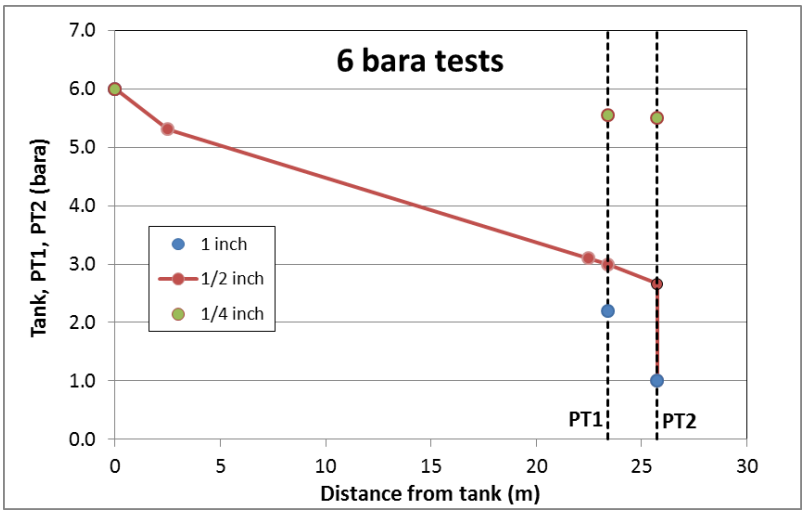

Figure 3: Pressure distribution for 6 bara tests. Vertical dashed lines show locations of pressure transducers PT1, PT2.

4 DISCHARGE SIMULATIONS

4.1 Input data

Table 5 below summarizes the discharge line parameters given as input to the engineering tool. All the resistance to the flow was modelled through the resistance factor K.

The discharge line was discretized with 401 steps with very small step size at the line exit. Such a small step size at the exit is required for choked flow simulations, in order to accurately model the sharp increase of the pressure gradient at this location.

Table 5: Discharge line parameters.

Element	Diameter (mm)	Length (m)	Grid steps	First step (m)	Last step (m)	K
Tanker pipework	45	2.5	25	0.1	0.1	335.85
Contraction	-	0.01	1	0.01	0.01	0.34
Vacuum insulated flexible hose	25.4	20	200	0.1	0.1	114.17
Electrically isolated pipe + MFM	25.4	0.9	9	0.1	0.1	5.16
Valve section + Flexible hose	25.4	2.35	106	0.1	0.001	17.53
Nozzle Contraction	-	0.01	10	0.001	0.001	0
Nozzle ending	25.4 or 12.7 or 6.35	0.01	50	0.001	6e-6	4.41

4.2 Results and discussion

Table 6 summarizes predicted versus reported by HSE [2] mass flow rates for all experimental cases and all models. Predicted mass flow rate for 6 bara-1/2 inch with constant density model nearly reproduces the experimental value of 265 g/s. This result was expected, because the discharge line resistance factors were estimated based on this particular experimental test case.

The constant density model generally overestimates the experimental mass flow rates by a maximum of 13.4 %. The HNEM model shows a maximum overestimation of 12.7 % and slight underestimation of -0.3 %. The classical HEM model shows a maximum overestimation of 9.6 % and underestimation of -3.3 %.

In general the constant density model produces the largest mass flow rates, followed by the HNEM model and last by the HEM model. This is an expected result, because in HNEM and HEM models density is decreased along the line compared to the constant density model and also because in HEM model density is decreased even more compared to HNEM, see Figure 4.

Table 7 shows predicted mass flow rates with HEM model, without a discharge line (no resistance factors). The significant effect of the discharge line in reducing the mass flow rate can be understood by comparing the results of Table 6 with those of Table 7. For 1 inch the mass flow rate without a discharge line is approximately 13 times larger.

Figure 5 shows predicted absolute pressure distribution along the discharge line for 6 bara tests with HEM model. The figure includes the measured pressures at transducers PT1 and PT2 for comparison. The agreement with the predictions is considered satisfactory.

Figure 6 shows predicted vapour quality distribution along the discharge line for the 6 bara tests with HEM model. It can be observed that only for the 1 inch case vapour appears and that this happens at approximately 25 m from the tank, i.e. inside the flexible hose prior to the exit nozzle. This explains the sharp density drop for HEM observed in Figure 4 close to the nozzle. Figure 6 also shows predicted vapour quality distribution along the discharge line for the 2 bara tests with HEM model. For this stagnation pressure vapour appears both for the 1 and ½ inch cases.

Table 6 Mass flow rates (g/s) predicted in this work with three different models and relative errors with respect to values reported by HSE in D3.6.

Nozzle diameter (mm)	Mass flow rate (g/s) and relative error (%) with respect to HSE							
	2 bara				6 bara			
	HSE	Const density	HNEM	HEM	HSE	Const density	HNEM	HEM
25.4	139.5	144.21 (3.4)	144.08 (3.3)	142.16 (1.9)	298	324.91 (9.0)	323.47 (8.5)	319.12 (7.1)
12.7	105.5	117.78 (11.6)	117.67 (11.5)	113.83 (7.9)	265	265.37 (0.1)	264.14 (-0.3)	256.20 (-3.3)
6.35		47.81	47.76	44.84	95	107.73 (13.4)	107.11 (12.7)	104.15 (9.6)

Table 7 Predicted mass flow rates (g/s) with HEM without a discharge line.

Nozzle diameter (mm)	Mass flow rate (g/s) with HEM, without discharge line	
	2 bara	6 bara
25.4	1804.9	4206.7
12.7	451.22	1051.7
6.35	112.81	262.92

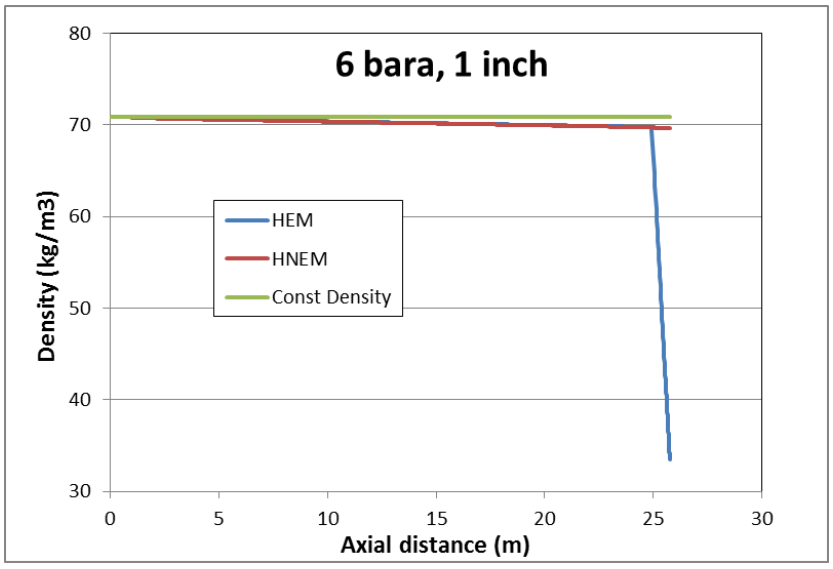

Figure 4: Predicted density distribution along the discharge line for 6 bara – 1 inch nozzle case with 3 models.

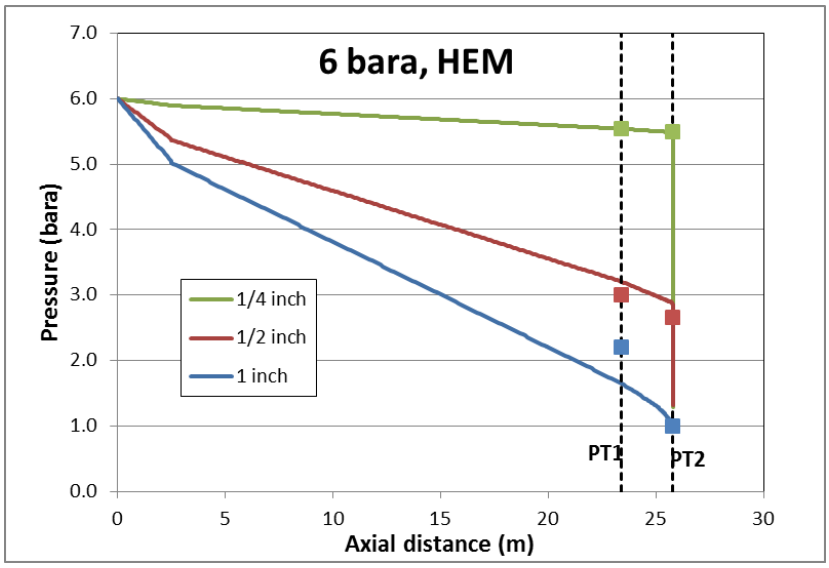

Figure 5: Predicted pressure distribution for 6 bara tests with HEM. Vertical dashed lines show locations of pressure transducers PT1, PT2. Square markers show the measured pressures PT1 and PT2.

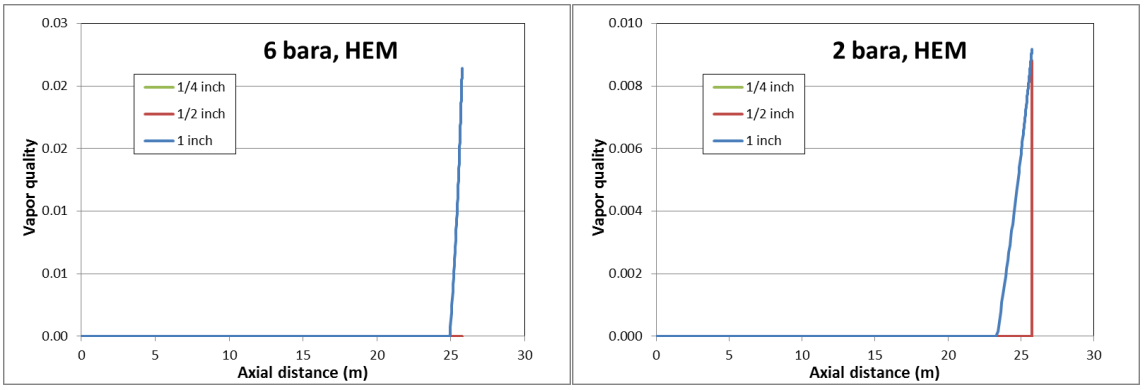

Figure 6: Predicted vapour quality distribution for 6 and 2 bara tests with HEM.

5 CONCLUSIONS

Steady state choked flow and adiabatic discharge simulations have been performed against the new LH_2 experiments performed by HSE within the PRESLHY project, involving stagnation pressures of 2 and 6 bara and 3 nozzle sizes (1/4, ½ and 1 inches).

Simulations were performed using the 1-d engineering tool developed by NCSRD. Discharge line resistance factors (K) were first estimated based on experimental test-11 (6 bara, ½ inch) for which experiments showed all liquid conditions up to the nozzle and then applied to all other simulated cases.

The performed analysis of the resistance factors revealed the dominant effect of the 20 m long vacuum insulated flexible hose creating approximately 2.22 bars pressure drop for test-11. Flexible hoses generally create significantly larger pressure drops compared to rigid pipes (an order of magnitude higher) and consequently could easier lead to two-phase conditions during depressurization along the discharge line. Therefore, as a suggestion to experimentalists, use of rigid pipes (downstream the storage tank) should be preferred during liquid cryogenic release experiments (not only LH_2), if the target is to have full liquid exit release conditions.

The performed analysis of the resistance factors K also revealed the large resistance factor of the pipework within the tanker (K = 336), information that could be useful for the industry.

Simulations were performed with 3 different two-phase models: HEM model, Constant density model and HNEM all liquid model.

The constant density model generally overestimated the experimental mass flow rates by a maximum of 13.4 %. The HNEM model showed a maximum overestimation of 12.7 % and slight underestimation of -0.3 %. The HEM model showed a maximum overestimation of 9.6 % and underestimation of -3.3 %.

Predicted pressure distribution along the discharge line for 6 bara tests with HEM model showed satisfactory agreement at pressure transducers PT1 and PT2 deployed during the experiments.

Without a discharge line HEM model was found to overestimate mass flow rates by 13 times, clearly indicating the importance of accounting for the discharge line in discharge simulations.

In view of the importance of the discharge line parameters in discharge simulations, it is suggested to experimentalists of future experiments to analyse and report estimated resistance factors for all parts of the discharge line.

6 ACKNOWLEDGEMENTS

The research leading to these results was financially supported by the PRESLHY project, which has received funding from the Fuel Cells and Hydrogen 2 Joint Undertaking under the European Union's Horizon 2020 research and innovation program under grant agreement No 779613. This Joint Undertaking receives support from the European Union's Horizon 2020 research and innovation programme, Hydrogen Europe and Hydrogen Europe research.

7 REFERENCES

1 Venetsanos A.G., Choked two-phase flow with account of discharge line effects, 8th International Conference on Hydrogen Safety, Adelaide, Australia, 24-26 Sept. 2019.
2 Lyons K., Coldrick S., Atkinson G., Summary of experiment series E3.5 (Rainout) results, PRESLHY EC-project deliverable D3.6, 2020, pp. 70.
3 Hall J., Hooker P., Coldrick S., Lyons K., Atkinson G., Royle M., Tooke A., HSE SD experimental summary for the characterisation, dispersion and electrostatic hazards of LH2 for the PRESLHY project, 9th Int. Conf. on Hydrogen Safety, 21-23 Sept. 2021, Edinburgh, UK.
4 Idel'chik I.E., Handbook of Hydraulic resistance, Coefficients of local resistance and of friction, 1966, pp. 517.
5 Batchelor, George K. (1967), An Introduction to Fluid Dynamics, Cambridge University Press, 634 pp.
6 Leachman J. W., Jacobsen R. T., Penoncello S. G., and Lemmon E. W., Fundamental Equations of State for Parahydrogen, Normal Hydrogen, and Orthohydrogen, J. Phys. Chem. Ref. Data, 38 (2009) 721-748.
7 Venetsanos A.G., Homogeneous non-equilibrium two-phase choked flow modelling, Int. J. of Hydrogen Energy, 43 (2018) 22715-22726.
8 Pinhasi GA, Ullmann A, Dayan A. Modelling of flashing two-phase flow. Rev Chem Eng. 2005; 21:133-264.
9 De Lorenzo M., Lafon Ph., Seynhaeve J.-M., Bartosiewicz Y., Benchmark of Delayed Equilibrium Model (DEM) and classic two-phase critical flow models against experimental data, Int. J. of Multiphase flow, 92 (2017) 112-130.
10 Riley, Kenneth Lloyd, "Flow Losses in Flexible Hose." (1967). LSU Historical Dissertations and Theses. 1313.